Least square migration of synthetic aperture data for towed streamer electromagnetic survey

Xiaolei TU[1] and Michael S. Zhdanov[1,2]; [1]University of Utah; [2]TechnoImaging*

Summary

Towed streamer electromagnetic (TSEM) survey is an efficient data acquisition technique capable of collecting a large volume of electromagnetic (EM) data over extensive areas rapidly and economically. However, the interpretation of TSEM data is still a challenging problem. We propose to solve this problem by migrating the optimal synthetic aperture (OSA) data for TSEM survey. We first represent the OSA data as the solution of Lippmann-Schwinger equation, and then demonstrate that the migration of OSA data is just the inner product of the backward-propagated and forward-propagated EM fields. The migration problem was solved iteratively within the general framework of the reweighted regularized conjugate gradient method. The proposed method was tested with two synthetic models. We also applied it to the dataset collected in the Barents Sea and revealed a resistive layer at a depth of about 500 m.

Introduction

A concept of the synthetic aperture (SA) is based on idea that a virtual source constructed from different actual sources with specific radiation patterns can steer the combined fields in the direction of an area of interest (*Fan et al.*, 2010; 2012; *Knaak et al.*, 2013). In the papers by *Yoon and Zhdanov* (2015) and *Zhdanov et al.* (2017) the authors introduced a concept of optimal synthetic aperture (OSA) by determining the optimal parameters of the SA data, which enhances the EM anomaly from a resistive region located in either deep or shallow marine environments. This method was also extended for rapid imaging of the TSEM survey data based on the concept of OSA. The OSA method could image the horizontal location of subsurface anomalies in a very rapid way without solving Maxwell's equations. However, the OSA images do not provide the physical property (i.e., conductivity or resistivity) of the anomaly. Furthermore, the SA or OSA images provide no depth information of the target since they did not take the survey geometry and frequency range into consideration.

In this paper, we have developed a new approach to imaging the TSEM data by performing migration directly on the OSA data. The developed novel method differs from the previous EM migration algorithms in three aspects. First, we apply the migration to the OSA data rather than to the observed EM data. Second, calculations of the migrated field (or the downward propagation of the time-reversed back-scattered fields) in the previous methods required a solution of Maxwell's equations, which is a nonlinear problem and needs considerable computation efforts. In our approach, the Lippmann-Schwinger equation corresponding to Maxwell's

system is linearized by introducing a new model parameter, which reduces the forward modeling computations significantly. Last but not the least, the recovery of the subsurface image of the new model parameter is obtained by a linear iterative solver, which we refer to as the least square migration after its seismic counterpart.

Integral representations of the OSA data

We consider a typical TSEM survey consisting of a towed bipole transmitter and a set of towed receivers. The transmitter generates a low-frequency EM field from positions with coordinates $\tilde{r}_j$, $j = 1, 2, \cdots, J$. According to *Yoon and Zhdanov* (2015), the OSA data $d_R^{(l)}$ at the virtual receiver position r_l are computed as:

$$d_R^{(l)} = \frac{d_A^{(l)}}{d_B^{(l)}} = \frac{\sum_{j=1}^{J} E_j^{(l)} w_j}{\sum_{j=1}^{J} E_j^{ref(l)} w_j}, \quad (1)$$

where $E_j^{(l)}$ denotes the interpolated field at virtual receiver position r_l corresponding to transmitter located at position $\tilde{r}_j$. $E_j^{ref(l)}$ represents the corresponding reference field for $E_j^{(l)}$, which generally depends on the offset $|r_l - \tilde{r}_j|$. w_j represents the OSA weight.

Consider a 3D geoelectrical model with background conductivity σ_b, and local inhomogeneity with varying conductivity, $\sigma = \sigma_b + \sigma_a$. The electromagnetic field generated by the OSA source in this model can be presented as the sum of the background and anomalous fields:

$$\tilde{\mathbf{E}} = \tilde{\mathbf{E}}^b + \tilde{\mathbf{E}}^a. \quad (2)$$

The integral equation for 3D EM forward modeling problem is written as:

$$\tilde{\mathbf{E}}^a(\mathbf{r}_l) = \iiint_V \mathbf{G}(\mathbf{r}_l|\mathbf{r}) \cdot \{\sigma_a(\mathbf{r})[\tilde{\mathbf{E}}^b(\mathbf{r}) + \tilde{\mathbf{E}}^a(\mathbf{r})]\} dv. \quad (3)$$

According to *Zhdanov* (2015), the anomalous field, $\tilde{\mathbf{E}}^a$, inside the inhomogeneous domain can be projected onto the background field by a scattering tensor, $\hat{\boldsymbol{\lambda}}$:

$$\tilde{\mathbf{E}}^a(\mathbf{r}_l) = \iiint_V \mathbf{G}(\mathbf{r}_l|\mathbf{r}) \cdot \{\sigma_a(\mathbf{r})[\hat{\mathbf{I}} + \hat{\boldsymbol{\lambda}}(\mathbf{r})] \cdot \tilde{\mathbf{E}}^b(\mathbf{r})\} dv, \quad (4)$$

where $\hat{\mathbf{I}}$ is the identity tensor.

The scattering tensor, $\hat{\boldsymbol{\lambda}}$, is called the electrical reflectivity tensor. In general, it's a 2nd order tensor with components represented by smoothly varying functions of the coordinates. We should note that, the scalar components of $\hat{\boldsymbol{\lambda}}(\mathbf{r})$ are complex functions depending nonlinearly on the anomalous conductivity, the background conductivity, and

Least square migration of synthetic aperture data for towed streamer electromagnetic survey

the excitation source. However, in a case of week-contrast media, $\hat{\boldsymbol{\lambda}}(\mathbf{r})$ is less dependent on the source and can be assumed to be a function of $\sigma_a(\mathbf{r})$ only. We assume assume, for simplicity, that $\hat{\boldsymbol{\lambda}}$ is a diagonal tensor. Under this assumption, a new model parameter, $\mathbf{m}(\mathbf{r})$, which we call the modified conductivity, is introduced:

$$\mathbf{m}(\mathbf{r}) = \sigma_a(\mathbf{r})[\hat{\mathbf{I}} + \hat{\boldsymbol{\lambda}}(\mathbf{r})]. \qquad (5)$$

By introducing the modified conductivity, $\mathbf{m}(\mathbf{r})$, the Lippmann-Schwinger equation can be linearized as follows:

$$\tilde{\mathbf{E}}^a(\mathbf{r}_l) = \iiint_V \mathbf{G}(\mathbf{r}_l|\mathbf{r}) \cdot \mathbf{m}(\mathbf{r}) \cdot \tilde{\mathbf{E}}^b(\mathbf{r}) dv, \qquad (6)$$

which can also be written in a compact form:

$$\mathbf{d} = \mathbf{Lm}, \qquad (7)$$

with the linear modeling operator, $\mathbf{L}$, and the data, $\mathbf{d}$, defined as followings:

$$\mathbf{L} = \iiint_V \mathbf{G}(\mathbf{r}_l|\mathbf{r}) \cdot \tilde{\mathbf{E}}^b(\mathbf{r}) dv, \qquad (8)$$

$$\mathbf{d} = [\tilde{\mathbf{E}}^a(\mathbf{r}_1) \quad \tilde{\mathbf{E}}^a(\mathbf{r}_2) \quad \cdots \quad \tilde{\mathbf{E}}^a(\mathbf{r}_L)]^T. \qquad (9)$$

Least square iterative migration of OSA data

As demonstrated in *Zhdanov* (2015), the migration is the action of the adjoint operator on the observed data. It follows that the migration image of modified conductivity, $\mathbf{m}^{mig}$, can be introduced as an action of the adjoint operator, $\mathbf{L}^*$, on the anomalous field data, $\mathbf{d}$:

$$\mathbf{m}^{mig} = \mathbf{L}^*\mathbf{d}. \qquad (10)$$

It can be proved that the migration operator can be written as follows:

$$\mathbf{L}^*\mathbf{d} = \tilde{\mathbf{E}}^{b*}(\mathbf{r}) \cdot \left[\iint_S \mathbf{G}^*(\mathbf{r}|\mathbf{r}')d(\mathbf{r}')ds'\right], \qquad (11)$$

where $\mathbf{G}^*(\mathbf{r}|\mathbf{r}')$ is the complex conjugate Green's tensor. Considering that the complex conjugate is equivalent to time reverse in time domain, the complex conjugate Green's tensor will result in the backward-propagation of EM fields in time domain. The term in square brackets in Equation (11) has a physical meaning of the backward propagation of the observed data back toward the subsurface media simultaneously from all the receivers. That is, all the receivers are considered as virtual sources, and the observed data are taken as the source function. If we denote this backward-propagated field as $\mathbf{E}^{BP}$:

$$\mathbf{E}^{BP}(\mathbf{r}) = \iint_S \mathbf{G}^*(\mathbf{r}|\mathbf{r}')d(\mathbf{r}')ds', \qquad (12)$$

the migration of EM anomalous field is then the inner product of the back-propagated and the forward-propagated fields:

$$\mathbf{m}^{mig} = \langle \mathbf{E}^{BP}(\mathbf{r}), \tilde{\mathbf{E}}^b(\mathbf{r}) \rangle. \qquad (13)$$

The migrated modified conductivity $\mathbf{m}^{mig}$ never exactly predicts the observed data in equation $\mathbf{d} = \mathbf{Lm}$. We can find

the only solution that minimizes the following regularized sum of the squared residuals:

$$p(\alpha) = \|\mathbf{Lm} - \mathbf{d}\|^2 + \alpha s(\mathbf{m}) = min. \qquad (14)$$

The solution of the above minimization problem is called *a least square migration* after its seismic counterpart. We should also note that, the gradient of the least square migration parametric functional without regularization is exactly the one step migration image $\mathbf{m}^{mig}$. The least square migration is thus an analog (for the case of modified conductivity, $\mathbf{m}$) of the generalized iterative migration method with regularization. The regularization term incorporates a priori information about the model, turning the ill-posed unconstrained inverse problem into a conditionally well-posed inverse problem (*Zhdanov*, 2015).

As a result of the diffusive nature of the low frequency EM fields, the migration image is always blurred and smoothed. In this situation, a more focused image with sharp boundaries of contrasting conductivity is often preferred. *Portniaguine and Zhdanov* (1999) introduced focusing stabilizers that made it possible to recover models with sharp boundaries and contrasts. In this paper, we consider the minimum support (MS) and minimum vertical gradient support (MVGS) stabilizers.

We base the solution of the minimization problem (14) on the re-weighted regularized conjugate gradient method (RRCG), which is easier to implement numerically (*Zhdanov*, 2015). The problem can be solved quickly in a few iterations thanks to the linearization of the Lippmann-Schwinger equation by introducing the modified conductivity.

Model study

Model 1
The developed methods and computer code were tested using computer generated data. Model 1 represents a three-layered geoelectrical model consisting of $300\ m$ sea-water layer with a conductivity of $3\ S/m$, the second $400\ m$ layer of $1\ S/m$, and a $0.1\ S/m$ half space of the basement. An L-shaped HC reservoir is embedded in the third layer with a depth of $1400\ m$ to the top as shown in Figures 1. We set the conductivity of the reservoir to be $10^{-3}\ S/m$, with a conductivity contrast ratio of 100 to the bedrocks. The towed streamer EM survey consists of 16 survey lines with $500\ m$ line spacing running in the east direction. The horizontal electric dipole transmitter with a moment of $1000\ Am$ is oriented in the east direction and is towed at a depth of $10\ m$ from $-10\ km$ to $10\ km$ to the east. The shot interval is also of $500\ m$, with the locations of the transmitters denoted by red dots in Figure 1. Twenty-five receivers with offsets from $1\ km$ to $7\ km$ are towed at a depth of $100\ m$ measuring the in-line electric fields at 8

Least square migration of synthetic aperture data for towed streamer electromagnetic survey
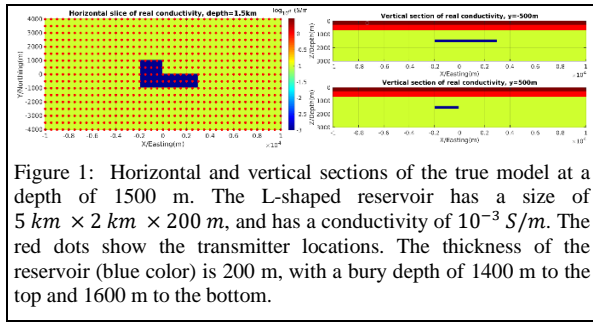
Figure 1: Horizontal and vertical sections of the true model at a depth of 1500 m. The L-shaped reservoir has a size of $5\ km \times 2\ km \times 200\ m$, and has a conductivity of $10^{-3}\ S/m$. The red dots show the transmitter locations. The thickness of the reservoir (blue color) is 200 m, with a bury depth of 1400 m to the top and 1600 m to the bottom.

frequencies between $0.1\ Hz$ and $3.1623\ Hz$. The data were contaminated with 2% Gaussian noise.
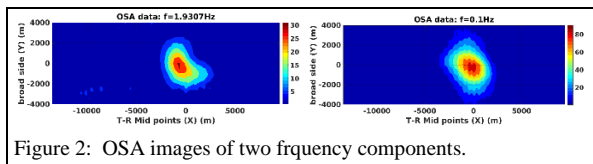
Figure 2: OSA images of two frquency components.

We have applied the OSA method (*Yoon and Zhdanov*, 2015; *Zhdanov et al.*, 2017) to the observed data. For every survey line, all the shots were combined to construct an OSA source for each virtual receiver location and per frequency. Figure 2 present the OSA data for all virtual receivers at 2 frequencies respectively. The approximate horizontal location of the reservoir is well recovered.
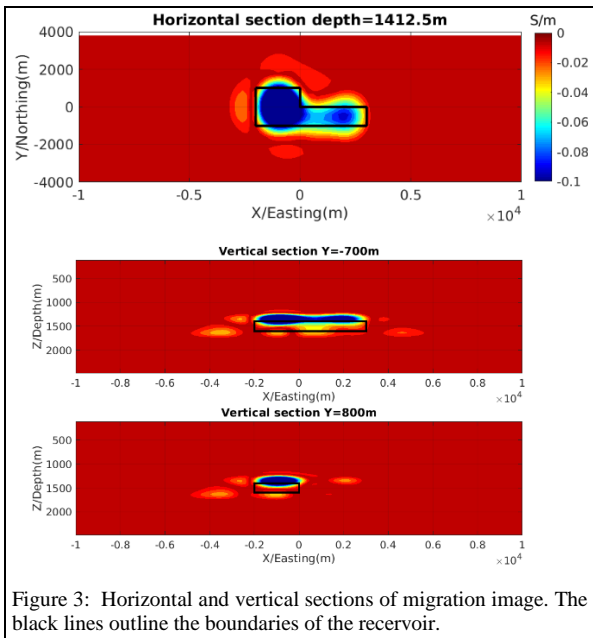
Figure 3: Horizontal and vertical sections of migration image. The black lines outline the boundaries of the recervoir.

We consider the OSA data as the observed data; and perform the least square migration directly on them. To deal with the diffusive nature of the EM fields, the MVGS stabilizer was applied for the regularization. The migrated modified conductivity was then normalized to the conventional conductivity. Figures 3 presents the migration images. One can see that, the location and shape of the reservoir are both well recovered horizontally and in the vertical direction.

Model 2
Model 2 is the SEG salt dome model. For convenience, we simplified the model by considering a two-layered background: a $300\ m$ sea-water layer with resistivity of $0.3\ Ohm \cdot m$, and a $6\ Ohm \cdot m$ half space of sediments. The resistivity of the salt dome is set to $1000\ Ohm \cdot m$ as shown in Figure 4. The survey configuration is the same as that in Model 1 except that the data are measured at 8 frequencies between $0.1\ Hz$ to $10\ Hz$. The synthetic data were first contaminated with 1% Gaussian noise and imaged using the OSA method. As illustrated in Figure 4, the OSA images locate the salt dome horizontally well.
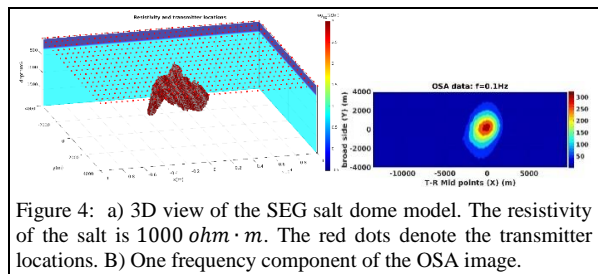
Figure 4: a) 3D view of the SEG salt dome model. The resistivity of the salt is $1000\ ohm \cdot m$. The red dots denote the transmitter locations. B) One frequency component of the OSA image.

The produced OSA images were then migrated with the least square migration with an MGS stabilizer, the migrated modified conductivity was also normalized to conductivity as in previous model study. One can see from Figure 5 that the migration image recovers the location and shape of the salt body reasonably well. This result illustrates that, the least square migration can be used to image subsurface anomalies from the OSA data.

Case study

In this section, we present the results of application of the developed least square migration method to the data collected by a TSEM survey conducted by PGS in the Barents Sea. The TSEM data used in our numerical study were collected at seven survey lines at six frequencies of 0.2, 0.4, 0.8, 1.4, 1.8, and 2.6 Hz. The 8700 m long EM streamer was towed at a depth of approximately 100 m below the sea surface. Twenty-three receivers with offsets between 2057 and 7752 m were selected. The electric current source was towed at a depth of approximately 10 m below the sea surface. Maps of observed inline electric field at a common

Least square migration of synthetic aperture data for towed streamer electromagnetic survey

offset of 3.4 km for all six frequencies components are shown in Figure 6.
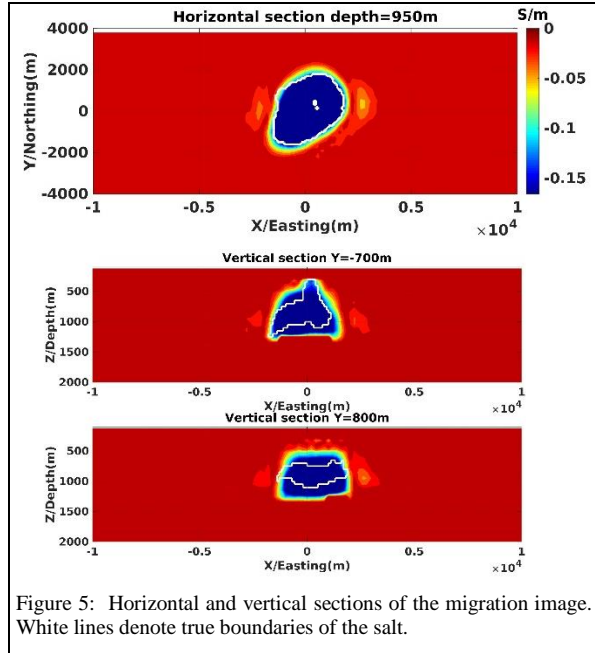
Figure 5: Horizontal and vertical sections of the migration image. White lines denote true boundaries of the salt.

We have applied the OSA method to the data for each frequency separately. The reference field was selected to be the set of the observed data generated by the remotely located transmitter for all frequencies, assuming that this field was least affected by the anomalous resistivity in the survey area. The OSA images are shown in Figure 6.
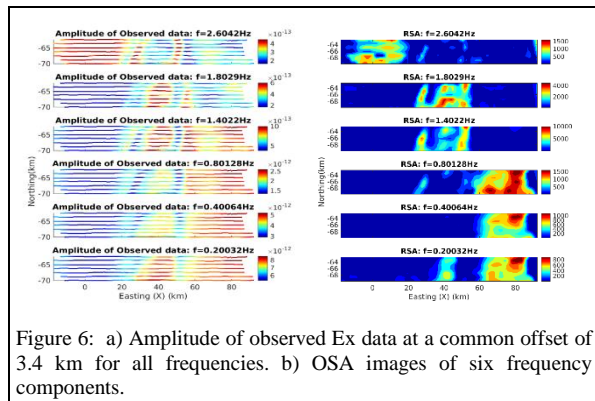
Figure 6: a) Amplitude of observed Ex data at a common offset of 3.4 km for all frequencies. b) OSA images of six frequency components.

We have migrated the OSA data using the developed least square migration algorithm with the VMGS focusing and horizontal maximum smoothing stabilizers. The background model was chosen to be a two-layered model consisting of 300 m sea-water layer with a resistivity of 0.33 $Ohm \cdot m$

and of a 5 $Ohm \cdot m$ sea-bed half space. The initial model was obtained by performing 1D inversion of the data for the common transmitter-receiver middle point. As can be seen from the migration images (Figure 7), there is a resistive layer at a depth of about 500 m. This layer bends up in the central part of the survey area, forming an anticline structure, which coincides with that of the OSA image.
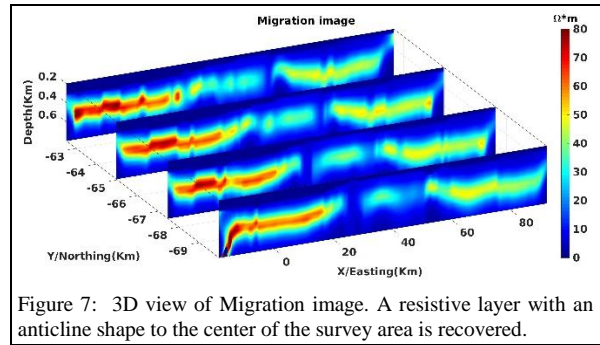
Figure 7: 3D view of Migration image. A resistive layer with an anticline shape to the center of the survey area is recovered.

Conclusions

We have developed a fast imaging method for interpretation of the TSEM data. The method consists of two steps. On the first step, we apply the OSA method to image the EM data observed at individual frequencies. On the second step, we use the migration transform of the OSA data jointly for all frequencies to generate the conductivity image of the sea-bottom formation. The migration is formulated as the inner product of the backward-propagated and forward propagated EM fields generated by the OSA source. By linearizing the Lippmann-Schwinger integral equation, we were able to develop a rapid solver for both the backward-propagation and forward modeling problems. We have also increased the sharpness of the inverse model by incorporating MS or MVGS regularization into the iterative migration. Synthetic test study demonstrated that the developed method could recover the horizontal location and the depth of the target reasonably well. The practical effectiveness of the method was also shown by imaging the TSEM data collected by PGS in the Barents sea.

Acknowledgements

REFERENCES

Fan, Y., R. Snieder, E. Slob, J. Hunziker, J. Singer, J. Sheiman, and M. Rosenquist, 2010, Synthetic aperture controlled source electromagnetics: Geophysical Research Letters, **37**, doi: https://doi.org/10.1029/2010GL043981.

Fan, Y., R. Snieder, E. Slob, J. Hunziker, J. Singer, J. Sheiman, and M. Rosenquist, 2012, Increasing the sensitivity of controlled-source electromagnetics with synthetic aperture: Geophysics, **77**, no. 2, E135–E145, doi: https://doi.org/10.1190/geo2011-https://doi.org/0102.1.

Knaak, A., R. Snieder, Y. Fan, and D. Ramirez-Mejia, 2013, 3D synthetic aperture and steering for controlled-source electromagnetics: The Leading Edge, **32**, 972–978, doi: https://doi.org/10.1190/tle32080972.1.

Portniaguine, O., and M. S. Zhdanov, 1999, Focusing geophysical inversion images: Geophysics, **64**, 874–887, doi: https://doi.org/10.1190/1.1444596.

Yoon, D., and M. S. Zhdanov, 2015, Optimal synthetic aperture method for marine controlled-source EM surveys: IEEE Geoscience and Remote Sensing Letters, **12**, 414–418, doi: https://doi.org/10.1109/LGRS.2014.2345416.

Zhdanov, M. S., 2015, Inverse theory and applications in Geophysics, 2nd ed.: Elsevier.

Zhdanov, M. S., D. Yoon, and J. Mattsson, 2017, Rapid imaging of towed streamer EM data using the optimal synthetic aperture method: IEEE Geoscience and Remote Sensing Letters, **14**, 262–266, doi: https://doi.org/10.1109/LGRS.2016.2637919.